

Bright X-ray and up-conversion nanophosphors annealed using encapsulated sintering agents for bioimaging applications

Hongyu Chen, Fenglin Wang, Thomas Moore, Bin Qi, Dino Sulejmanovic, Shiou-Jyh Hwu, O. Thompson Mefford, Frank Alexis, and Jeffrey N. Anker

Electronic Supplementary Information

Table of contents: This supporting information includes and figures addressing phosphor characterization in terms of spectroscopy, X-ray diffraction, electron microscopy, and toxicity.

Table S1. Crystal domain size of $Gd_2O_2S:Eu$ after doped with 7.6 mol% sintering agents p 2

Figure S1. XRD powder patterns of (A) $Gd_2O(CO_3)_2 \cdot H_2O:Eu$, (B) crystalized $Gd_2O(CO_3)_2 \cdot H_2O:Eu$ during annealing in the glycerol, (C) crystalized $Gd_2O(CO_3)_2 \cdot H_2O:Eu$ with encapsulated NaF during annealing in the glycerol. p 3

Figure S2. TEM images of monodispersed (A) NaF doped $Gd_2O_2S:Tb$ with protective layer, (B) NaF doped $Y_2O_2S:Yb/Tm$ with protective layer, (C) $Gd_2O_2S:Tb$ without NaF doping, (D) $Y_2O_2S:Yb/Tm$ without NaF doping. p 3

Figure S3. Comparison of X-ray excited luminescence of different types of (A) $Gd_2O_2S:Eu$ phosphors (1 mg/mL) and (B) $Gd_2O_2S:Tb$ (1 mg/mL). p 4

Figure S4. Fluorescence emission spectra under 480 nm excitation for (A) $Gd_2O_2S:Eu$ with and without 7.6 mol% NaF doping and (B) $Gd_2O_2S:Tb$ with and without 7.6 mol% NaF doping. p 4

Figure S5. Effect of different NaF-doping concentration on the X-ray excited optical luminescence intensity at 620 nm for $Gd_2O_2S:Eu$ nanophosphors. p 5

Figure S6. Comparison of upconversion luminescence of different types of $Y_2O_2S:Yb/Tm$ phosphors (0.25 mg/mL). p 5

Figure S7. Chemical reaction scheme for synthesis of PEG-FA conjugated nanophosphors. p 6

Figure S8. Primary mechanism of amine functionalization on nanophosphors by (3-Aminopropyl)triethoxysilane (APTES). p 6

Figure S9. Luminescence intensity of nanophosphors at different stages of surface modification. p 7

Figure S10. TEM images of PEG-FA functionalized $Gd_2O_2S:Eu$ (A) and $Y_2O_2S:Yb/Er$ (B) with NaF doping. p 7

Figure S11. Zeta potential of the nanophosphors at different stages of surface modification. p 8

Figure S12. Cytotoxicity test of NaF doped $Gd_2O_2S:Eu$ and $Y_2O_2S:Yb/Er$. Viability at 0 $\mu g/mL$ is defined as 100%. p 8

Figure S13. Total luminescence counts from colloidal solution of nanophosphors injected 1 cm deep into chicken breast. (A) X-ray nanophosphors, with and without NaF sintering agent, excited by X-rays, and (B) up-conversion nanophosphors, with and without NaF sintering agent, excited by 980 nm light. p 9

Table S1. Crystal domain size (from XRD) and luminescence enhanced factor at 620 nm of Gd₂O₂S:Eu after doped with 7.6 mol% various sintering agent.

Sintering agents (7.6 mol%)	Crystal domain size (nm)	Enhanced factor
NaF	46	12.5
KF	45	12.1
NaCl	37	8.3
KCl	36	8.1
NaBr	28	3.5
KBr	30	3.8
NaI	21	1.4
KI	21	1.2
Na ₂ CO ₃	34	5.2
K ₂ CO ₃	34	5.0
No sintering agent	21	Defined as 1.0

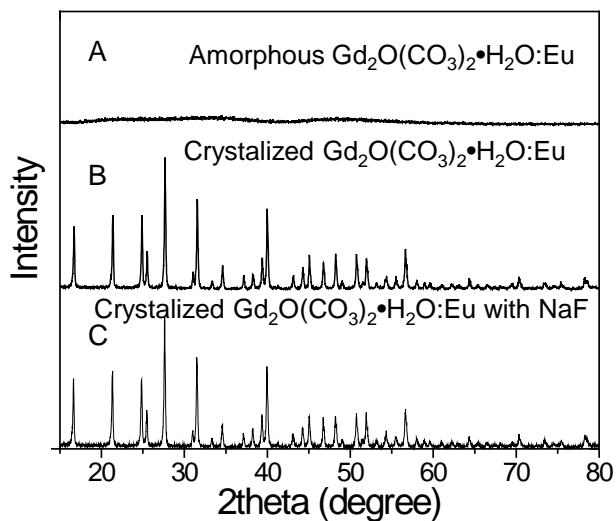


Figure S1. XRD powder patterns of (A) Gd₂O(CO₃)₂•H₂O:Eu, (B) crystallized Gd₂O(CO₃)₂•H₂O:Eu during annealing in the glycerol, (C) crystallized Gd₂O(CO₃)₂•H₂O:Eu with encapsulated NaF during annealing in the glycerol.

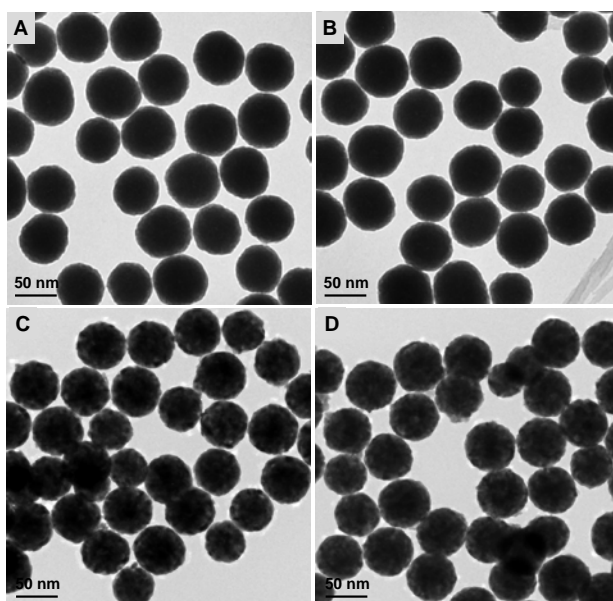


Figure S2. TEM images of monodispersed (A) NaF-doped Gd₂O₂S:Tb with protective layer, (B) NaF-doped Y₂O₂S:Yb/Tm with protective layer, (C) Gd₂O₂S:Tb without NaF doping, (D) Y₂O₂S:Yb/Tm without NaF doping.

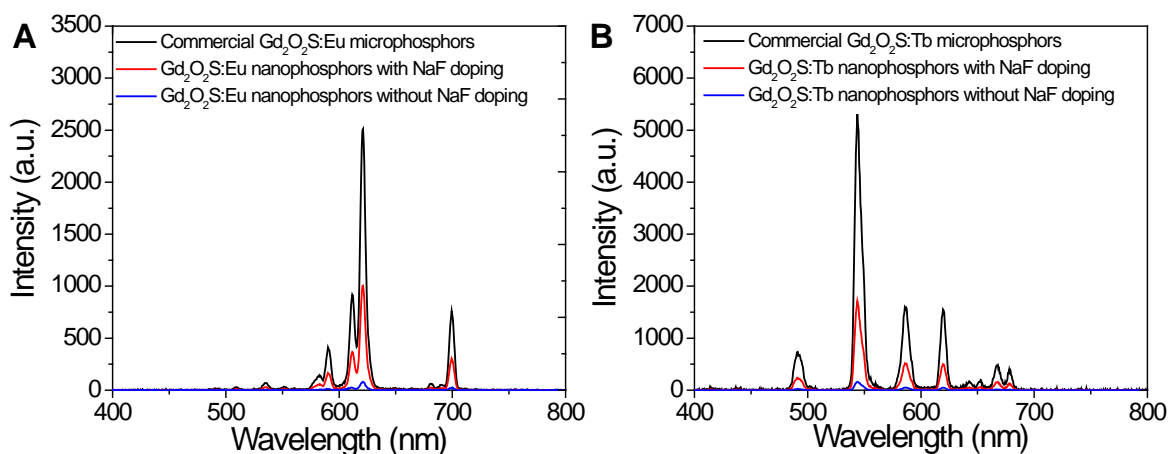


Figure S3. Comparison of X-ray excited luminescence of different types of (A) Gd₂O₂S:Eu phosphors (1 mg/mL) and (B) Gd₂O₂S:Tb (1 mg/mL).

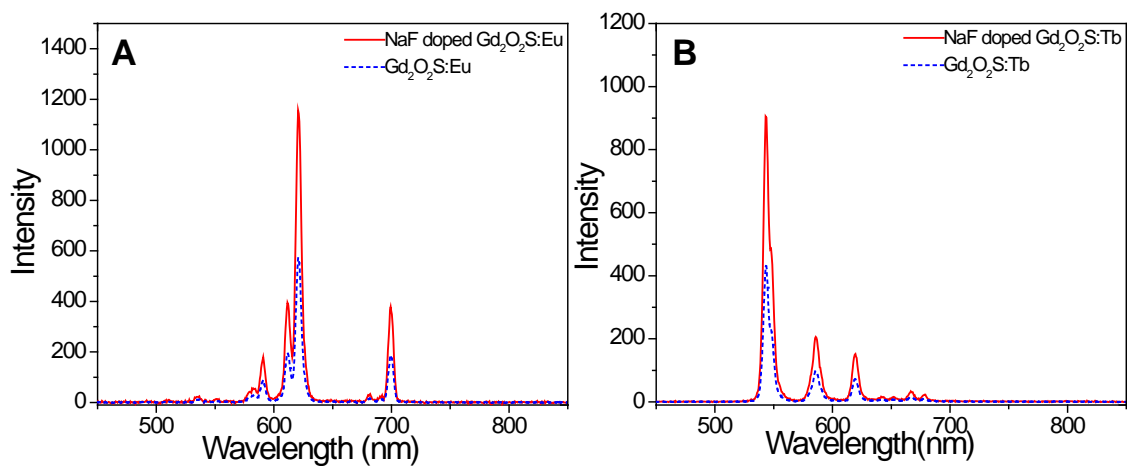


Figure S4. Fluorescence emission spectra, using 480 nm excitation, for (A) Gd₂O₂S:Eu with and without 7.6 mol% NaF doping and (B) Gd₂O₂S:Tb with and without 7.6 mol% NaF doping.

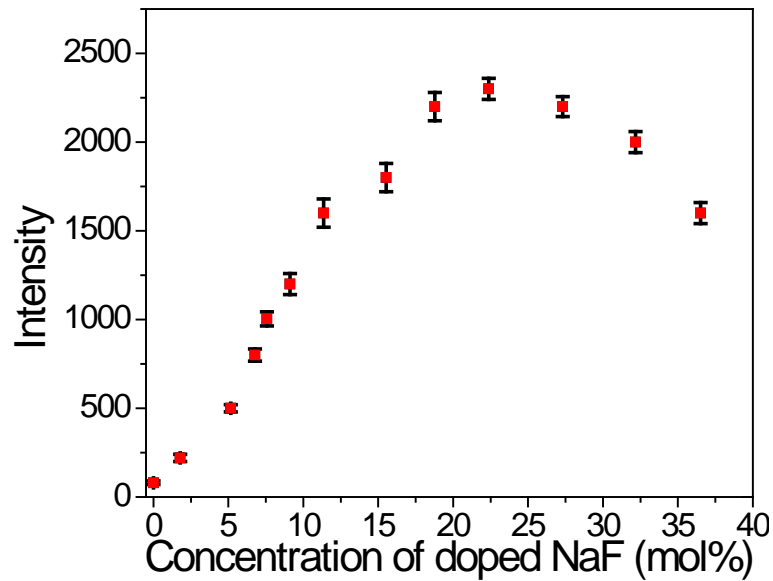


Figure S5. Effect of NaF-doping concentration on the X-ray excited optical luminescence intensity at 620 nm for $Gd_2O_2S:Eu$ nanophosphors.

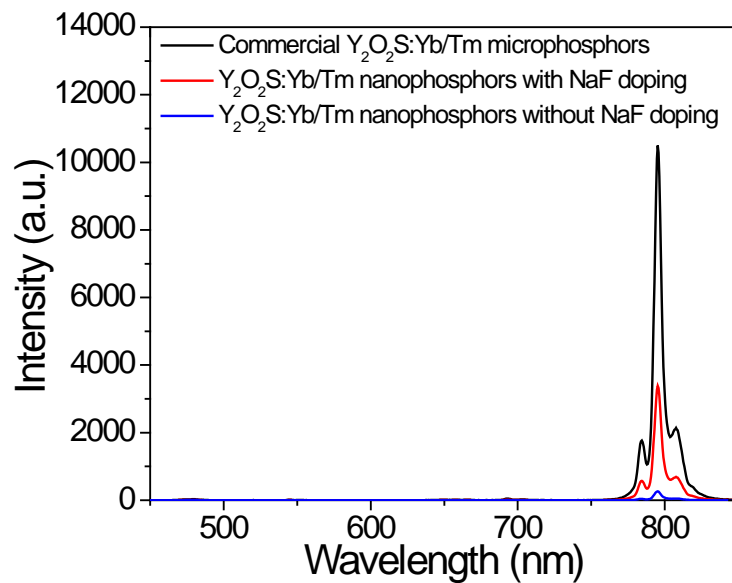


Figure S6. Comparison of upconversion luminescence of different types of $Y_2O_2S:Yb/Tm$ phosphors (0.25 mg/mL).

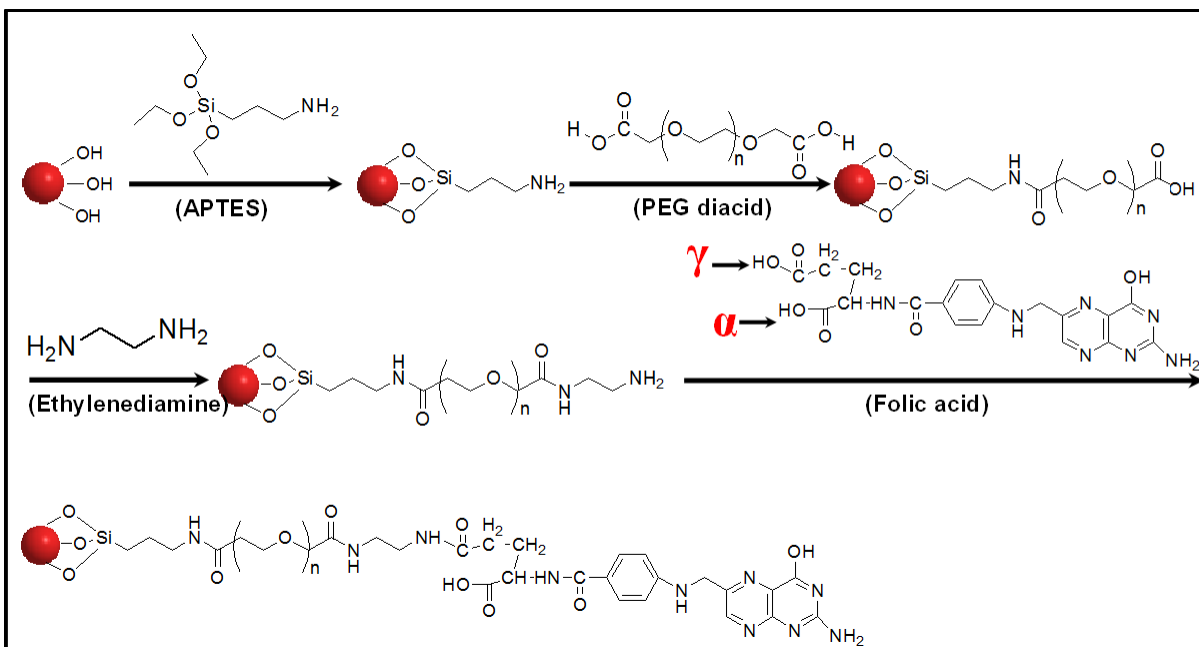


Figure S7. Chemical reaction scheme for synthesis of PEG-FA conjugated nanophosphors.

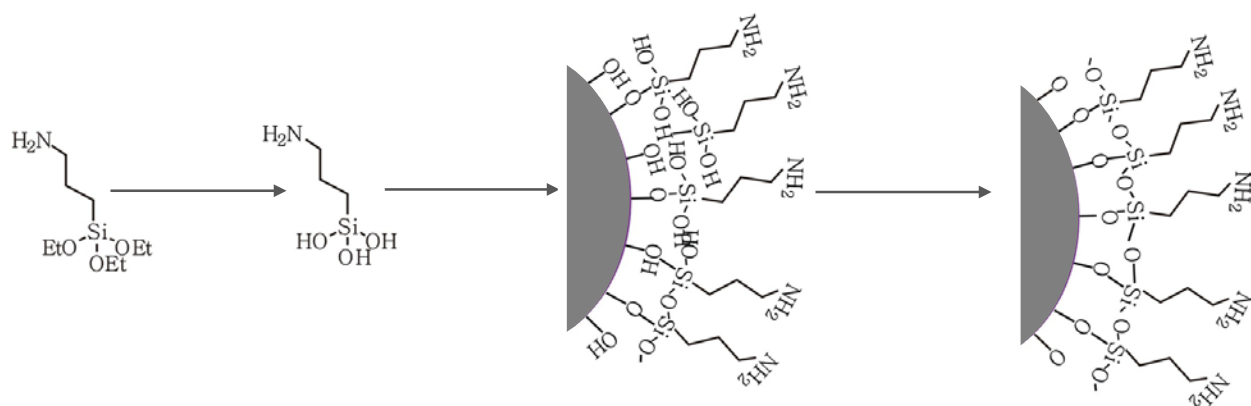


Figure S8. Primary mechanism of amine functionalization on nanophosphors by (3-Aminopropyl)triethoxysilane (APTES).

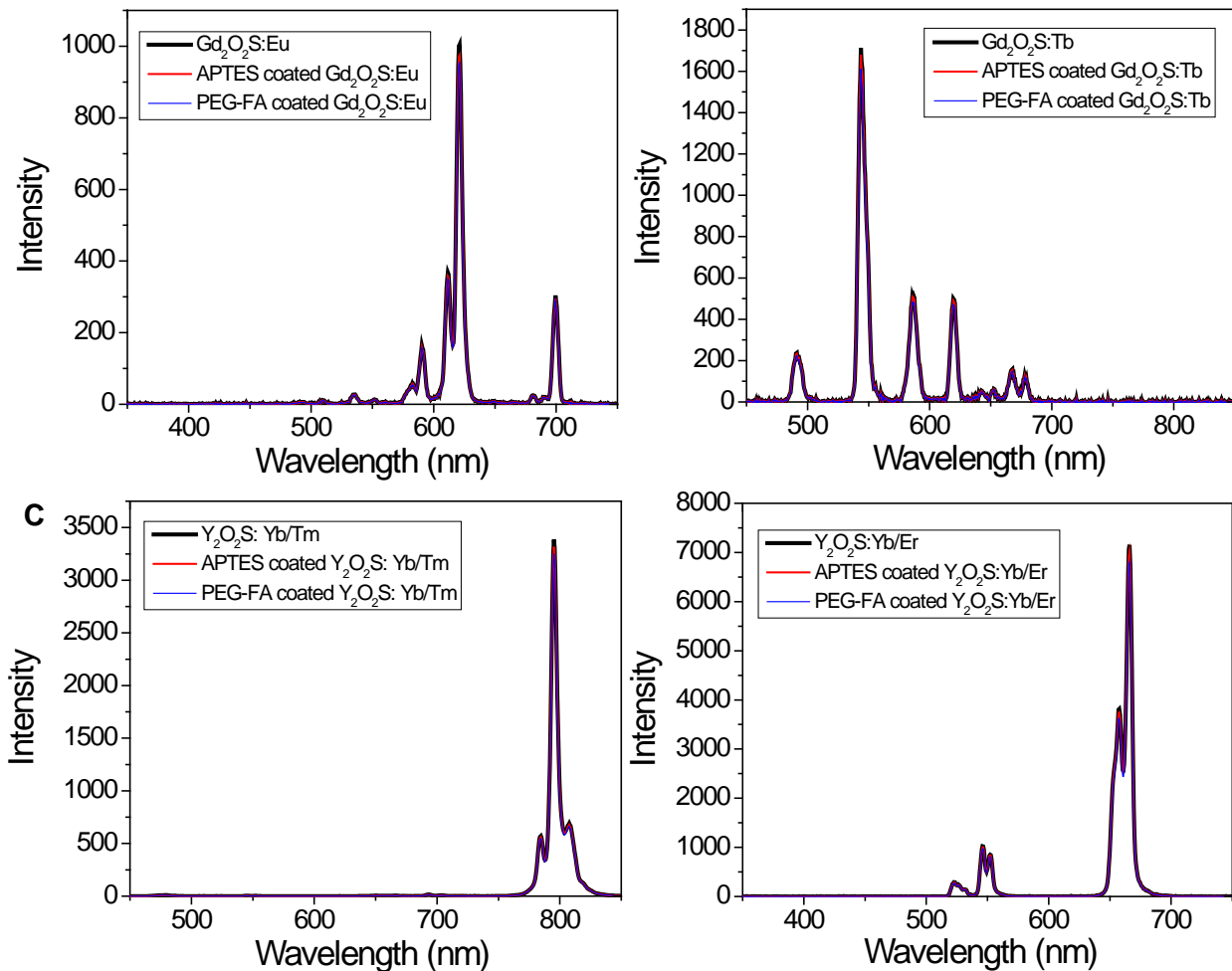


Figure S9. Luminescence intensity of nanophosphors at different stages of surface modification.

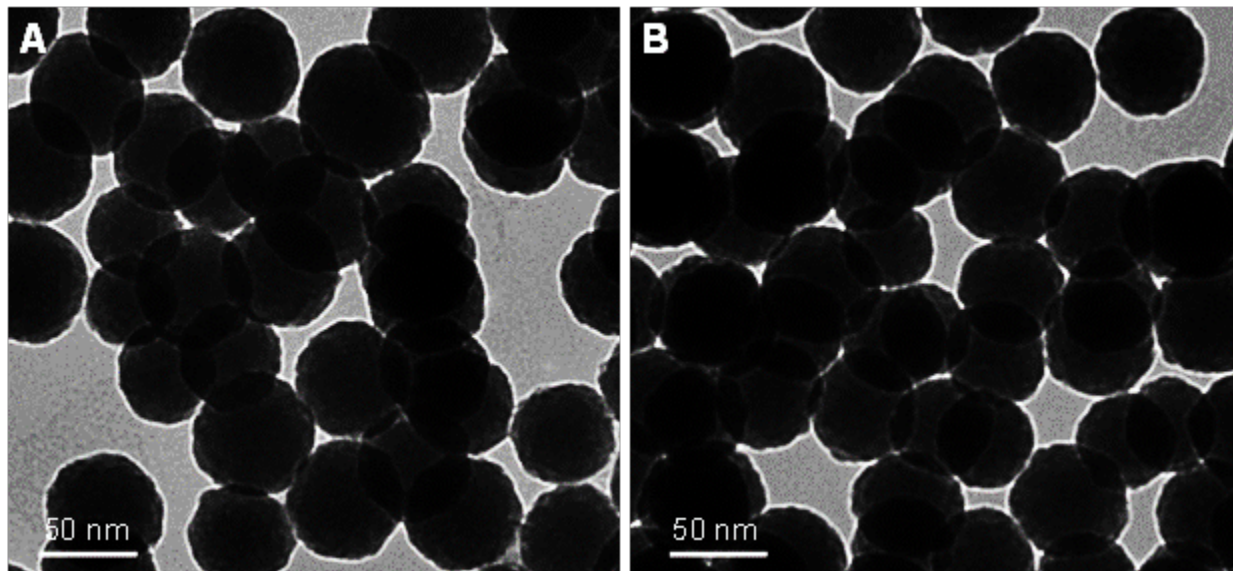


Figure S10. TEM images of PEG-FA functionalized $Gd_2O_2S:Eu$ (A) and $Y_2O_2S:Yb/Er$ (B) with NaF doping.

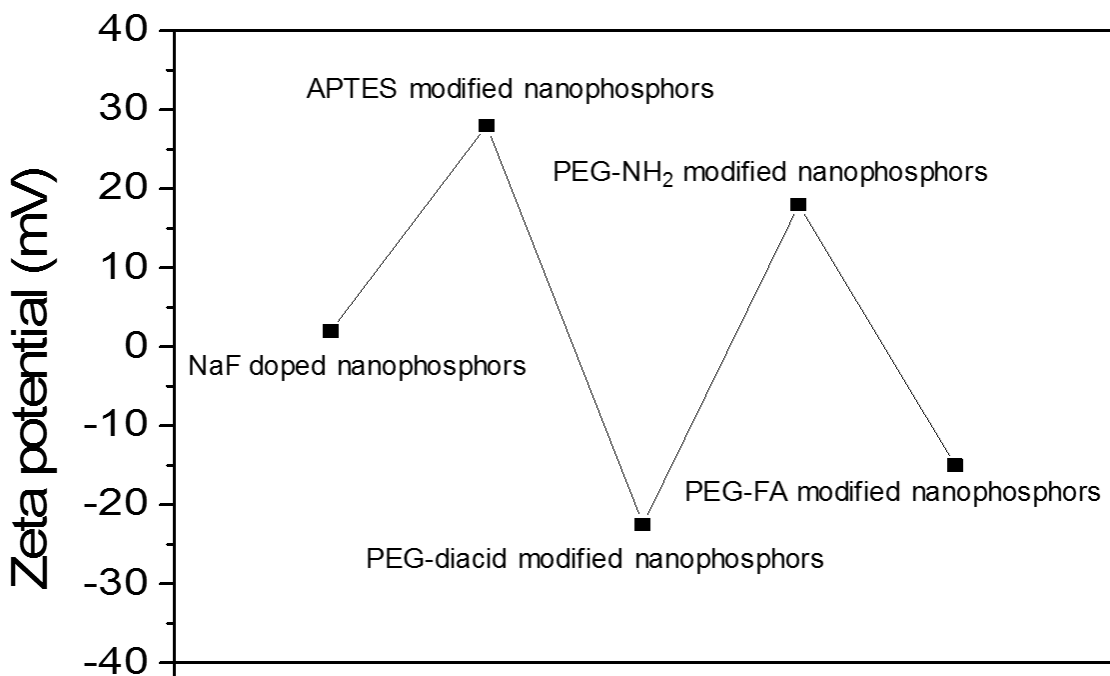


Figure S11. Zeta potential of the nanophosphors at different stages of surface modification.

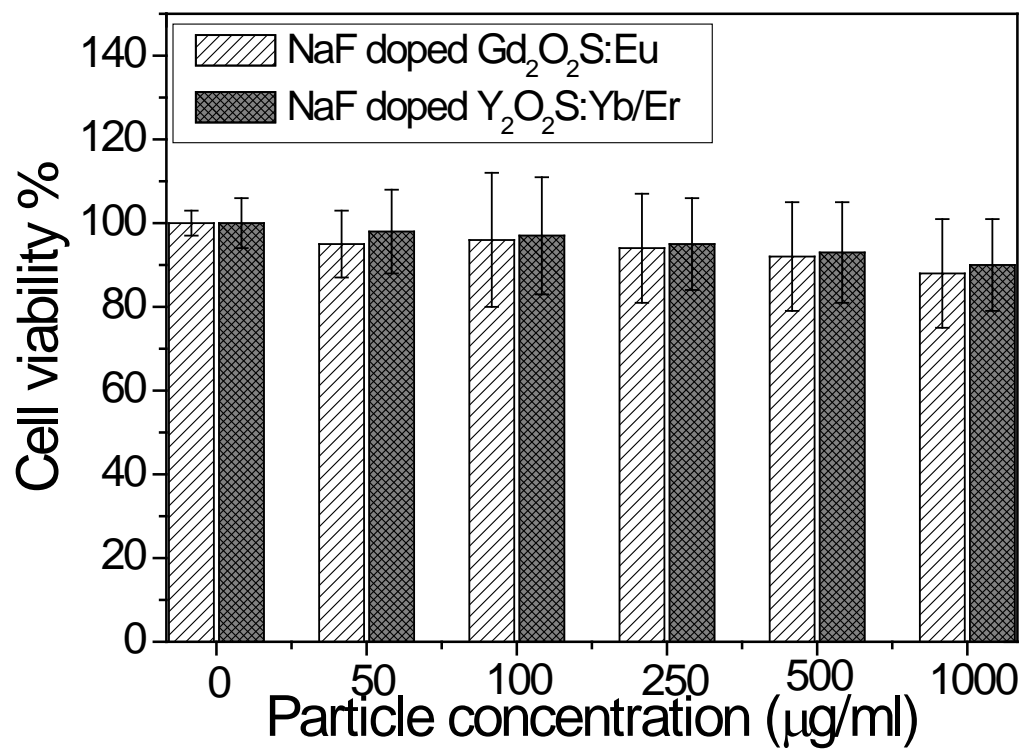


Figure S12. Cytotoxicity test of NaF-doped Gd₂O₂S:Eu and Y₂O₂S:Yb/Er. Viability at 0 µg/mL is defined as 100%.

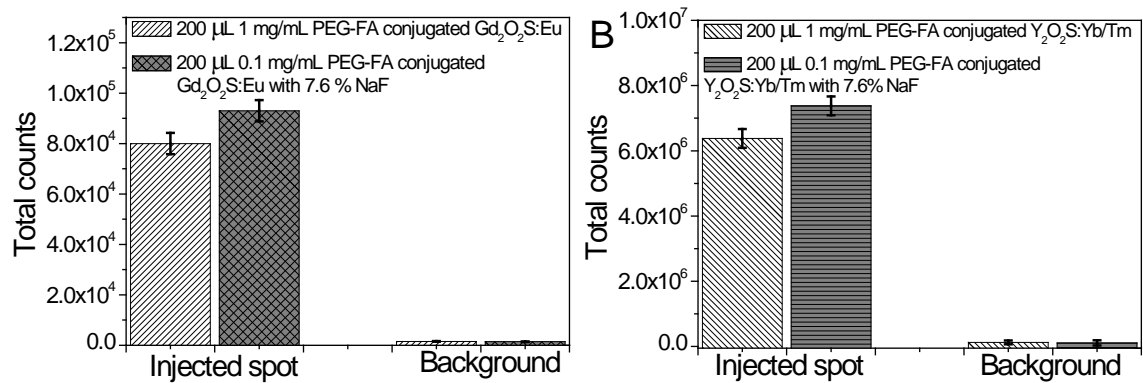


Figure S13. Total luminescence counts from colloidal solution of nanophosphors injected 1 cm deep into chicken breast. (A) X-ray nanophosphors, with and without NaF sintering agent, excited by X-rays, and (B) up-conversion nanophosphors, with and without NaF sintering agent, excited by 980 nm light.